Journal of Computational Physics 228 (2009) 4823–4835

Contents lists available at ScienceDirect

Journal of Computational Physics

journal homepage: www.elsevier.com/locate/jcp

Symmetry boundary conditions

R.E. Denton *, Y. Hu

Dartmouth College, Department of Physics and Astronomy, 6127 Wilder Lab, Hanover, NH 03755, United States

ARTICLE INFO

Article history:
Received 11 November 2008
Received in revised form 19 March 2009
Accepted 24 March 2009
Available online 1 April 2009

MSC:
35Rxx
76M20
76W05

PACS:
42.25.Gy
46.15.−x
87.16.−A

Keywords:
Numerical methods
Plasma physics
Boundary conditions
Curvilinear coordinates
MHD
Reduced MHD
Hybrid simulations

ABSTRACT

A simple approach to energy conserving boundary conditions using exact symmetries is described which is especially useful for numerical simulations using the finite difference method. Each field in the simulation is normally either symmetric (even) or antisymmetric (odd) with respect to the simulation boundary. Another possible boundary condition is an antisymmetric perturbation about a nonzero value. One of the most powerful aspects of this approach is that it can be easily implemented in curvilinear coordinates by making the scale factors of the coordinate transformation symmetric about the boundaries. The method is demonstrated for magnetohydrodynamics (MHD), reduced MHD, and a hybrid code with particle ions and fluid electrons. These boundary conditions yield exact energy conservation in the limit of infinite time and space resolution. Also discussed is the interpretation that the particle charge reverses sign at a conducting boundary with boundary normal perpendicular to the background magnetic field.

1. Introduction

A particular set of boundary conditions can have an important effect on the results of plasma simulations [11,3,25,26]. An important class of boundary conditions is that of energy conserving boundary conditions. Energy conserving boundary conditions are sometimes appropriate for laboratory plasmas [2]. Energy conserving boundary conditions are not ideal for all problems. For instance, in simulation of space plasmas, it is often desirable for energy to radiate out of the system simulating an open boundary [12,14,5]. But it is difficult to find boundary conditions that let all of the various wave modes escape out of the simulation region, and such boundary conditions are often much less stable than energy conserving boundary conditions. Typically when numerical codes "blow up" (that is, values of quantities get very large), it happens in such a way that the computational energy grows. Related to this, the most stable boundary conditions are typically energy conserving. For some

* Corresponding author.
E-mail address: rdjcp@rdenton.fastem.com (R.E. Denton).

0021-9991/$ - see front matter © 2009 Elsevier Inc. All rights reserved.
doi:10.1016/j.jcp.2009.03.033

applications, such as the study of Alfvén waves that are guided along the magnetic field, the boundary condition across the magnetic field should not matter, and an energy conserving boundary condition may be convenient. Finally, energy conservation is one of the best tests of a numerical code, and energy conserving boundary conditions make it easier to check that the total simulation energy is constant.

Here, we demonstrate a simple method to determine and implement energy conserving boundary conditions using symmetries about the boundaries. The boundary conditions appropriate for Cartesian coordinates can be used for curvilinear coordinates if the scale factors describing those coordinates are taken to be symmetric about the boundary. We illustrate our method for several different sets of plasma physics equations. While not all aspects of the boundary conditions we describe here are new, we believe that our clear explanation of how to implement them (which we have not found elsewhere) will be helpful to researchers using fluid or particle simulations.

For the sake of completeness, we have included in Section 5 a description of symmetry boundary conditions for reduced MHD. Much of this material can be found in Ref. [9]. Here we have a more complete description of the boundary conditions for all fields (Table 4) using a notation consistent with that used in the rest of this paper.

2. Symmetry basics

In Table 1, we list the symmetries used in this paper. We use (+) to indicate that a field value is symmetric relative to a particular boundary, and (−) to indicate that a field value is antisymmetric relative to that boundary. "Symmetric" here means that the field is even across the boundary; that is, $f(x_0+\delta x)=f(x_0-\delta x)$, where x is the coordinate normal to the boundary at $x=x_0$, and $\delta x = x - x_0$. In this case, the first derivative of f is zero at the boundary. Antisymmetry means that the field is odd across the boundary; that is, $f(x_0+\delta x)=-f(x_0-\delta x)$, from which it is clear that an antisymmetric field has $f(x_0)=0$. The symbol $(\pm)$ indicates a mixed symmetry, not purely symmetric or antisymmetric, which as we will see is undesirable. The last three symbols in Table 1 are used only in Section 5. The notation 0 indicates that a field is identically zero everywhere, or an operator that yields zero when acting on a field. The symbol (+0) indicates (+) symmetry, but the value of the function turns out to be equal to zero at x_0. In other words, $f \propto c_2\delta x^2 + c_4\delta x^4 \ldots$ close to the boundary (the c_0 coefficient of the Taylor expansion is zero). The symbol $(\delta-)$ indicates an antisymmetric perturbation about a constant value, $f(x_0+\delta x)-f(x_0)=-(f(x_0-\delta x)-f(x_0))$, from which we get $f(x_0+\delta x)=f(x_0)-(f(x_0-\delta x)-f(x_0))=2f(x_0)-f(x_0-\delta x)$. This results in an inflection point with the second derivative of f equal to zero at the boundary.

These symmetries are useful for implementing boundary conditions in finite difference simulation codes. In finite difference simulations, boundary conditions are typically implemented using "buffer" or "ghost" grid points beyond the boundary. For instance, if a boundary is at grid point $i=n$, a zero value Neumann boundary condition (zero slope) can be implemented by use of grid points beyond the boundary with $f_{n+\Delta i}=f_{n-\Delta i}$, where $\Delta i = i - n$. Then any centered finite difference formula for the first derivative at $x=x_n$ will yield zero. For instance, the second order accurate formula for the first derivative at grid point i, $(f_{i+1}-f_{i-1})/(2\Delta x)$, is equal to zero at $i=n$ if $f_{n+1}=f_{n-1}$. While we have a finite difference method in mind (the finite volume method is discussed toward the end of this section), these symmetries can also be useful for defining the possible modes (sine or cosine) used in a spectral or pseudospectral method. Note that these symmetries really represent the effect of image charges/currents/flows to give the corresponding boundary condition.

While the simplest description of the (−) and (+) boundary conditions might be that the value of a field or one of its derivatives is zero at the boundary, the symmetry boundary conditions really imply more: (+) symmetry implies that all odd order derivatives, d^nf/dx^n with n odd, are zero, and (−) symmetry implies that all even order derivatives, d^nf/dx^n with n even, are zero. The distinction might not be all that important for a second order spatially accurate code, but for higher order schemes (we typically use fourth order spatial differencing), it makes a difference.

To see how exact symmetries lead to energy conservation, consider the one dimensional problem for the energy $\mathcal{E}$ in terms of a flux density S,

$$\frac{\partial \mathcal{E}}{\partial t}+\frac{\partial S}{\partial x}=0, \tag{1}$$

for a finite difference simulation with grid points at i = 1–N. Now assume that the first derivative at grid point i is evaluated using a difference formula

Table 1
Definitions of symmetry symbols.

Symbol	Definition
(+)	Symmetric, $f(x_0+\delta x)=f(x_0-\delta x)$
(−)	Antisymmetric, $f(x_0+\delta x)=-f(x_0-\delta x)$ [Note: $f(x_0)=0$]
$(\pm)$	Mixed symmetry, no simple relation between $f(x_0+\delta x)$ and $f(x_0-\delta x)$
0	Used to indicate a field that is everywhere identically zero
(+0)	Symmetric with zero value at x_0, $f(x_0+\delta x)=f(x_0-\delta x)$ and $f(x_0)=0$
$(\delta-)$	Antisymmetric perturbation, $f(x_0+\delta x)-f(x_0)=-(f(x_0-\delta x)-f(x_0))$

$$\left.\frac{\partial S}{\partial x}\right|_i = \sum_{j=1}^{M} c_j (S_{i+j} - S_{i-j}), \tag{2}$$

where for our purposes the c_j can have any values. For instance, the second order accurate formula has $M = 1$ with $c_1 = 1/(2\Delta x)$. The key point is that Eq. (2) involves an antisymmetric combination (reversed sign) of S_{i+j} and S_{i-j}. The total energy, $\sum_{i=1}^{N} \mathcal{E}$, will be conserved if $\sum_{i=1}^{N} \partial S/\partial x = 0$. Thus for energy conservation, we want

$$\sum_{i=1}^{N} \sum_{j=1}^{M} c_j (S_{i+j} - S_{i-j}) = 0. \tag{3}$$

This sum will certainly be equal to zero if each term in the sum over j is zero, that is, if

$$\sum_{i=1}^{N} (S_{i+j} - S_{i-j}) = 0. \tag{4}$$

Now consider only the left boundary at $x_{1/2} = x_1 - \Delta x/2$. Neglecting the terms at the right boundary near $i = N$, the left term in Eq. (4) is

$$\sum_{i=1}^{N} S_{i+j} = \sum_{i=1}^{N} S_i - \sum_{k=1}^{j} S_k. \tag{5}$$

For instance, for $j = 1$, there is no S_1 term coming from S_{i+1} for any $i = 1$ to N, and this has been subtracted off in Eq. (5). The right sum in Eq. (4) is (again neglecting boundary effects at the far boundary near $i = N$),

$$\sum_{i=1}^{N} S_{i-j} = \sum_{i=1}^{N} S_i + \sum_{k=1}^{j} S_{1-k}. \tag{6}$$

That is, there are extra terms that come from beyond the boundary at $x_{1/2}$, for instance, S_0 from $S_{i-j} = S_0$ for $i = j = 1$. If we subtract Eq. (6) from Eq. (5), we get for Eq. (4) (neglecting terms at the far boundary)

$$\sum_{i=1}^{N} (S_{i+j} - S_{i-j}) = -\sum_{k=1}^{j} (S_k + S_{1-k}). \tag{7}$$

If S is asymmetric across the boundary at $x_{1/2}$, then $S_{1-k} = -S_k$ and Eq. (7) will yield zero so that the total energy will be conserved. With the symmetry method, each of the fields in the model equations is defined with a consistent symmetry across the boundary, so that if an energy equation Eq. (1) can be derived for the interior region, it will also be applicable at and across the boundary. The net result is that the energy will be conserved to the same extent that it is in the interior, limited only by the spatial resolution of the simulation.

If $f = g$, the symmetry of f must be equal to that of g in order for the identity to be valid at the boundary with no discontinuities. Furthermore, if $f = gh$, the symmetry of f will be the symmetry of the product of the symmetries of g and h where (+) acts like +1, and (−) acts like −1. That is,

$$(+)(+) = (+), \tag{8}$$
$$(+)(-) = (-), \tag{9}$$
$$(-)(+) = (-), \tag{10}$$
$$(-)(-) = (+). \tag{11}$$

For the most part we have in mind coordinates systems that are orthogonal [1]. The numerical characteristics of such a coordinate system are fully specified by the scale factors h_k (for component direction k) that convert the change in a particular coordinate dq_k to distance in real space ds through $ds_k = h_k dq_k$. For instance, for cylindrical coordinates r, ϕ, and z, the scale factors h_k are 1, r, and 1, respectively. For such a coordinate system, the vector fields can be expressed in terms of the three coordinate directions. Relative to a particular boundary, a vector quantity has three symmetries, and we indicate this by use of a column symmetry vector. A vector with all three components symmetric would be denoted by

$$\begin{bmatrix} (+) \\ (+) \\ (+) \end{bmatrix}. \tag{12}$$

A derivative across a boundary has (−) symmetry. By this, we mean that the derivative operator modifies the symmetry just as if it were a field using the rules in Eqs. (8)–(11). This can be easily understood by considering a function at $x_0 = 0$ where increasing x crosses the boundary. If the function is symmetric about $x = 0$, $f(x) = c_0 + c_2 x^2 \ldots$, then $\partial f/\partial x \sim 2c_2 x$ is antisymmetric with respect to x. Therefore $\partial/\partial x$ reverses the symmetry of the function upon which it acts and can be thought of as having (−) symmetry. Similarly, if the function is antisymmetric about $x = 0$, $f(x) =$

$c_1x + c_3x^3 \ldots, \partial f/\partial x \sim c_1 + 3c_3x^2$ is symmetric about the boundary. However, a gradient orthogonal to the boundary normal has (+) symmetry. For instance, consider a field $f = c_0 + c_1y$, and note that it is symmetric with respect to x. The partial derivative with respect to y will be $\partial f/\partial y = c_1$ on both sides of $x = 0$. Therefore, with respect to $x, \partial f/\partial y$ is also symmetric with respect to x, and $\partial/\partial y$ therefore has (+) symmetry relative to the x boundary. In three dimensions, a boundary is a plane. The orientation of the boundary can be indicated by specifying the direction normal to the boundary, $\boldsymbol{n}$. For a boundary with boundary normal $\boldsymbol{n}$ in the direction of the first coordinate $\boldsymbol{e}_1$ (that is, for the boundary in a plane extending in the directions of the second and third components that is crossed when moving in the direction of the first coordinate),

$$\boldsymbol{\nabla} = \begin{bmatrix} (-) \\ (+) \\ (+) \end{bmatrix}, \tag{13}$$

while for the boundary with boundary normal in the direction of the second coordinate,

$$\boldsymbol{\nabla} = \begin{bmatrix} (+) \\ (-) \\ (+) \end{bmatrix}. \tag{14}$$

Now we can see why the symmetry boundary conditions for Cartesian coordinates can be used without modification for generalized orthogonal coordinates, as long as the scale factors of the transformation are taken to have (+) symmetry. For instance, from a normalized version of Ampere's Law, $\mathbf{J} = \boldsymbol{\nabla} \times \mathbf{B}$, the first component of the current is in generalized coordinates,

$$J_1 = \frac{1}{h_2h_3}\left(\frac{\partial}{\partial x_2}(h_3B_3) - \frac{\partial}{\partial x_3}(h_2B_2)\right), \tag{15}$$

where the x_k are the generalized coordinates. However, if all the scale factors h_k have (+) symmetry, the overall symmetry of the equation is not altered from that in Cartesian coordinates,

$$J_1 = \frac{\partial B_3}{\partial x_2} - \frac{\partial B_2}{\partial x_3}, \tag{16}$$

(because multiplication of a (+) symmetry quantity does not change the symmetry).

With generalized coordinates, Eq. (1) generalizes to

$$\frac{\partial \mathcal{E}}{\partial t} + \boldsymbol{\nabla} \cdot \mathbf{S} = 0, \tag{17}$$

The energy integral must then include the volume element; that is, the total energy generalizes to

$$\sum_{i=1}^{N} \mathcal{E}_i V_i, \tag{18}$$

where V_i is the volume element associated with grid point i. Then the quantity that must equal zero for energy conservation is

$$\sum_{i=1}^{N} V_i \boldsymbol{\nabla} \cdot \mathbf{S}|_i = 0. \tag{19}$$

Using the generalized coordinate form for $\boldsymbol{\nabla} \cdot \mathbf{S}$,

$$\boldsymbol{\nabla} \cdot \mathbf{S} = \frac{1}{h_1h_2h_3}\left[\frac{\partial}{\partial q_1}(S_1h_2h_3) + \frac{\partial}{\partial q_2}(S_2h_3h_1) + \frac{\partial}{\partial q_3}(S_3h_1h_2)\right], \tag{20}$$

and the fact that $V_i \propto h_{1i}h_{2i}h_{3i}$ for evenly spaced generalized coordinates, the h_k factors in front of the derivatives in Eq. (20) cancel with V_i in Eq. (19) (apart from a constant) so that Eq. (17) takes the form of Eq. (1) across each boundary. (To preserve the order of accuracy of the difference formulas, generalized coordinates should be evenly spaced; stretching of the dimensions can be done by varying the h_k.)

While we have only tested the energy conserving symmetry method for simulations using orthogonal coordinates, the method should also work for simulations with non-orthogonal coordinates (see, e.g. Ref. [24]). A coordinate transformation can be described by a metric tensor, g_{ij}, that upon (matrix) multiplication switches covariant and contravariant components back and forth [13]. To apply our method, all the components of the metric tensor should have (+) symmetry.

It is essential to understand that the symmetries in an equation are totally unrelated to any ordinary signs that may appear in that particular equation. Therefore, in Faraday's law, $\partial \boldsymbol{B}/\partial t = -\boldsymbol{\nabla} \times \boldsymbol{E}$, the minus sign on the right-hand side of the equation is irrelevant for determining the symmetries of the vector quantities. Also, $\partial/\partial t$ does not change symmetry across a boundary, so this operator has (+) symmetry.

A centered difference finite difference equation written in conservative form can be written in terms of fluxes $\mathcal{F}$ crossing the cell boundaries (see, e.g. Ref. [28]). What we mean is that Eq. (1) can be written

$$\Delta\mathcal{E} = \mathcal{F}_{i-1/2} - \mathcal{F}_{i+1/2}, \tag{21}$$

where $\mathcal{F}_{i-1/2}$ is the flux of energy crossing the grid point boundary $i-1/2$ from grid point $i-1$ to grid point i (integrated over time Δt and the dimensions perpendicular to x). Eq. (21) then expresses the fact that the change in the energy is equal to the energy flux coming in through the left boundary minus the energy flux going out through the right boundary. For instance, consider the second order accurate finite difference representation of Eq. (2),

$$\left.\frac{\partial S}{\partial x}\right|_i = \frac{S_{i+j} - S_{i-j}}{2\Delta x}. \tag{22}$$

Using this difference formula, the energy flux is

$$\mathcal{F}_{i+1/2} = \frac{\Delta t}{2\Delta x}(S_i + S_{i+1}), \tag{23}$$

just an integrated average of the flux density S.

A formulation in terms of fluxes crossing boundaries is often called the finite volume technique, and it can be used also for curved systems [15]. If an equation for energy is solved (Eq. (1); to solve, for instance, for a fluid pressure) and the flux of energy from the boundary surface is set equal to zero, then the energy will automatically be conserved. Why then would symmetry boundary conditions be useful? For one thing, it is not always practical to use an energy equation like Eq. (1). For instance, in the LFM magnetospheric global MHD code [18], an equation for plasma energy is solved for the sum of the kinetic and pressure energy, excluding the magnetic energy. This prevents accuracy problems in the very low plasma beta region (region with a low value for the ratio of thermal to magnetic pressure) close to the Earth. With this scheme, the coupling term between the plasma and fields is still $\mathbf{J}\cdot\mathbf{E}$, and conditions on the fields will still be necessary at the boundary. Having consistent symmetries across the boundary for $\mathbf{E}$ and $\mathbf{B}$ will insure that the crucial step in the derivation of energy conservation, $\nabla\cdot(\boldsymbol{E}\times\boldsymbol{B}) = \boldsymbol{B}\cdot\nabla\times\boldsymbol{E} - \boldsymbol{E}\cdot\nabla\times\boldsymbol{B}$, is satisfied across the boundary to the same extent that it is in the interior.

Even if an equation for the total energy is used, it will still be necessary to define values of fields beyond the boundary if a high order scheme is used for the calculation of the fluxes; this is because the fluxes in the interior (that are not zero) will depend on the values outside the simulation domain (at least using ghost values beyond the boundary as is commonly done). For instance, the LFM code uses an 8th order spatial accurate scheme that requires values 3.5 grid points away from a grid cell boundary in order to calculate the flux. The symmetries described here are one way to evaluate the derivatives in the finite difference equations or the fluxes in a finite volume scheme so as to preserve the order of the numerical accuracy, even at the boundary. If the symmetries are consistent, then all the equations will be solved in a manner that is consistent with the boundary conditions, and subsidiary relations, like adiabaticity of pressure evolution (which won't be automatic if an equation for total energy is used), will also be solved accurately to the greatest extend possible consistent with the grid resolution.

In our formulation, each boundary direction is independent and the boundary symmetries are evaluated directly across the boundary. Ref. [21] describes another interesting approach that uses inversion symmetry through the origin. Such inversion symmetry could be created within our framework by a combination of symmetries at a corner of the simulation. (This is somewhat different from Nevins et al.'s [21] technique which has inversion about the midpoint of a boundary surface.)

3. Energy conserving boundary conditions for MHD

The normalized MHD equations are

$$\rho\frac{d\boldsymbol{v}}{dt} = -\nabla p + \boldsymbol{J}\times\boldsymbol{B}, \tag{24}$$

$$\frac{\partial\rho}{\partial t} + \nabla\cdot(\rho\boldsymbol{v}) = 0, \tag{25}$$

$$\frac{\partial p}{\partial t} + \gamma\nabla\cdot(p\boldsymbol{v}) + (1-\gamma)\boldsymbol{v}\cdot\nabla p = (\gamma-1)\eta J^2, \tag{26}$$

$$\boldsymbol{J} = \nabla\times\boldsymbol{B}, \tag{27}$$

$$\frac{\partial\boldsymbol{B}}{\partial t} = -\nabla\times\boldsymbol{E}, \tag{28}$$

$$\boldsymbol{E} = -\boldsymbol{v}\times\boldsymbol{B} + \eta\boldsymbol{J}, \tag{29}$$

where $\boldsymbol{B}$ is normalized to the background magnetic field B_0, ρ is normalized to the background mass density ρ_0, $\boldsymbol{v}$ is normalized to the background Alfvén speed $V_A = B_0/\sqrt{\mu_0\rho_0}$, where μ_0 is the permeability of free space, and p is normalized to $\rho_0 V_A^2$.

The first step toward deriving energy conserving boundary conditions is to derive an energy equation. This is found by dotting (24) with $\boldsymbol{v}$, (28) with $\boldsymbol{B}$, and adding the two resulting equations to (26). The result is

$$\frac{\partial}{\partial t}\mathcal{E} = -\nabla\cdot\boldsymbol{S}, \tag{30}$$

$$\mathcal{E} = \frac{\rho\boldsymbol{v}^2}{2} + \frac{p}{\gamma-1} + \frac{\boldsymbol{B}^2}{2}, \tag{31}$$

$$\boldsymbol{S} = \left(\frac{\rho\boldsymbol{v}^2}{2} + \frac{\gamma p}{\gamma-1}\right)\boldsymbol{v} + \boldsymbol{E}\times\boldsymbol{B}, \tag{32}$$

where $\mathcal{E}$ is the total energy density and $\boldsymbol{S}$ is the energy flux density. To derive energy conserving boundary conditions, we need to have $\boldsymbol{S}\cdot\boldsymbol{n} = 0$ at the boundary. (That is, aside from periodic boundary conditions, which are automatically energy conserving given the fact that Eqs. (30)–(32) are in conservative form.) While it might be possible in principle to have individual terms within $\boldsymbol{S}$ contribute nonzero flux across the boundary but cancel out so that the total flux across the boundary is zero, in practice, we will need to set each term contributing to $\boldsymbol{S}\cdot\boldsymbol{n}$ equal to zero. Unless $p = 0$ at the boundary, it is clear that we need $\boldsymbol{v}\cdot\boldsymbol{n} = 0$. We also need $(\boldsymbol{E}\times\boldsymbol{B})\cdot\boldsymbol{n} = 0$. This can be accomplished with $\boldsymbol{E}\times\boldsymbol{n} = 0$ or $\boldsymbol{B}\times\boldsymbol{n} = 0$. If $\boldsymbol{n} = \boldsymbol{e}_1$, where $\boldsymbol{e}_1$ is the unit vector in the first coordinate direction (that is, the boundary is crossed by motion in the direction of the first coordinate), other possible energy conserving boundary conditions are $E_2 = B_2 = 0$ or $E_3 = B_3 = 0$.

We now assume that there is a background magnetic field in the $\boldsymbol{e}_1$ direction ($\boldsymbol{b}_0 = \boldsymbol{B}_0/B_0 = \boldsymbol{e}_1$), and consider boundary conditions for boundaries with $\boldsymbol{n} = \boldsymbol{e}_1$ and $\boldsymbol{n} = \boldsymbol{e}_2$. Recall that we are possibly considering curved coordinates.

3.1. Insulator boundary for boundary normal $\boldsymbol{n}$ parallel to $\boldsymbol{b}_0$

For boundary normal $\boldsymbol{n} = \boldsymbol{e}_1$,

$$\nabla = \begin{bmatrix}(-)\\(+)\\(+)\end{bmatrix}. \tag{33}$$

It is natural to make ρ, p, and $B_1 \sim B_0$ symmetric across the boundary since these quantities have nonzero equilibrium values. We require $v_1 = \boldsymbol{v}\cdot\boldsymbol{e}_1 = 0$ to make the flux density of pressure and kinetic energy equal to zero. If there is no inherent difference between the $\boldsymbol{e}_2$ and $\boldsymbol{e}_3$ directions, that limits us to two possible conditions for the electromagnetic fields, $\boldsymbol{E}\times\boldsymbol{n} = 0$ or $\boldsymbol{B}\times\boldsymbol{n} = 0$.

We consider first $\boldsymbol{B}\times\boldsymbol{n} = 0$. We call this an insulating boundary condition. As we will see, an electric field is allowed in the plane of the boundary and no current is allowed into it, consistent with the properties of an insulator. Using the equations of MHD, Eqs. (24)–(29), we require that the symmetries of all terms on the left side of an equation be equal to the symmetries of all terms on the right side. Now we have

$$\boldsymbol{B} = \begin{bmatrix}(+)\\(-)\\(-)\end{bmatrix}. \tag{34}$$

From Ampere's Law Eq. (27),

$$\boldsymbol{J} = \nabla\times\boldsymbol{B} = \begin{bmatrix}(-)\\(+)\\(+)\end{bmatrix}\times\begin{bmatrix}(+)\\(-)\\(-)\end{bmatrix} = \begin{bmatrix}(-)\\(+)\\(+)\end{bmatrix}, \tag{35}$$

where we mean by $\boldsymbol{J} = [\mathcal{S}]$ that $\boldsymbol{J}$ has the $[\mathcal{S}]$ symmetries. Noting that

$$\boldsymbol{v}\cdot\nabla = \begin{bmatrix}(-)\\(+)\\(+)\end{bmatrix}\cdot\begin{bmatrix}(-)\\(+)\\(+)\end{bmatrix} = (+) = \frac{\partial}{\partial t}, \tag{36}$$

we use the momentum equation Eq. (24),

$$\rho\frac{d\boldsymbol{v}}{dt} = -\nabla p + \boldsymbol{J}\times\boldsymbol{B} \quad\rightarrow \tag{37}$$

$$(+)\begin{bmatrix}(-)\\(?)\\(?)\end{bmatrix} = \begin{bmatrix}(-)\\(+)\\(+)\end{bmatrix}(+) + \begin{bmatrix}(-)\\(+)\\(+)\end{bmatrix}\times\begin{bmatrix}(+)\\(-)\\(-)\end{bmatrix}, \tag{38}$$

to find

$$\boldsymbol{v} = \begin{bmatrix} (-) \\ (+) \\ (+) \end{bmatrix}. \tag{39}$$

We use Ohm's Law Eq. (29),

$$\boldsymbol{E} = -\boldsymbol{v} \times \boldsymbol{B} + \eta \boldsymbol{J} \quad \rightarrow$$
$$\begin{bmatrix} (?) \\ (?) \\ (?) \end{bmatrix} = \begin{bmatrix} (-) \\ (+) \\ (+) \end{bmatrix} \times \begin{bmatrix} (+) \\ (-) \\ (-) \end{bmatrix} + (+) \begin{bmatrix} (-) \\ (+) \\ (+) \end{bmatrix}, \tag{40}$$

to find

$$\boldsymbol{E} = \begin{bmatrix} (-) \\ (+) \\ (+) \end{bmatrix}, \tag{41}$$

so as we claimed earlier, there can be an electric field within the boundary ((+) symmetry for E_2 and E_3 in Eq. (41)), but no current into the boundary ((−) symmetry for J_1 in Eq. (35)).

These symmetries are summarized in Table 2 under the $\boldsymbol{n} = \boldsymbol{e}_1$ Insulator column. Using similar analysis, it is easy to verify that Eqs. (25), (26), and (28) will all also have consistent symmetries. The authors used this boundary condition in a study of magnetospheric toroidal (azimuthally oscillating) Alfvén waves in dipole geometry [9].

It is possible to use different but related equations such as $\nabla \cdot \mathbf{B} = 0$ and $\nabla \cdot \mathbf{J} = 0$ to derive some of the same results.

3.2. Hard wall perfect conducting boundary with $\boldsymbol{n} = \boldsymbol{e}_1$

Now we consider a perfect conductor boundary with $\boldsymbol{n} = \boldsymbol{e}_1$ (boundary crossed in the direction of $\boldsymbol{b}_0$). In this case the components of $\boldsymbol{E}$ perpendicular to $\boldsymbol{n}$ will be zero, but the components of $\boldsymbol{B}$ perpendicular to $\boldsymbol{n}$ can be nonzero. The astute reader may have noticed that for the insulator boundary, all the vectors had the symmetry of ∇ or that of $(-)\nabla$, that is, one of the two symmetries

$$\begin{bmatrix} (-) \\ (+) \\ (+) \end{bmatrix}, \quad \begin{bmatrix} (+) \\ (-) \\ (-) \end{bmatrix}. \tag{42}$$

(The symmetry of the component in the direction of $\boldsymbol{n}$ was reversed from the symmetries of the other components.) This property was necessary to make the symmetries of all the equations come out totally consistent. In the case of the conductor boundary, the symmetries will not come out entirely consistent because the magnetic field is in the direction of $\boldsymbol{n}$. If we try to make B_1 have $(-)$ symmetry at the boundary, there will be large currents near the boundary that will lead to flows that erode B_1.

The best solution to this problem seems to be to require all components of $\boldsymbol{E}$ and $\boldsymbol{v}$ to be zero at the boundary. This results in a "line tied" boundary condition. The field lines are fixed (tied down) at the boundary because the components of $\boldsymbol{v}$ per-

Table 2
Symmetries for energy conserving boundary conditions in MHD.

Field	$\boldsymbol{n} = \boldsymbol{e}_1$		$\boldsymbol{n} = \boldsymbol{e}_2$
	Insulator	Conductor	Conductor
ρ, p, h_1, h_2, h_3	(+)	(+)	(+)
$\mathbf{V}$	$\begin{bmatrix} (-) \\ (+) \\ (+) \end{bmatrix}$	$\begin{bmatrix} (-) \\ (+) \\ (+) \end{bmatrix}$	$\begin{bmatrix} (+) \\ (-) \\ (+) \end{bmatrix}$
$\boldsymbol{B}$	$\begin{bmatrix} (+) \\ (-) \\ (-) \end{bmatrix}$	$\begin{bmatrix} (+) \\ (+) \\ (+) \end{bmatrix}$	$\begin{bmatrix} (+) \\ (-) \\ (+) \end{bmatrix}$
$\boldsymbol{J}$	$\begin{bmatrix} (-) \\ (+) \\ (+) \end{bmatrix}$	$\begin{bmatrix} (+) \\ (\pm) \\ (\pm) \end{bmatrix}$	$\begin{bmatrix} (-) \\ (+) \\ (-) \end{bmatrix}$
$\boldsymbol{v}$	$\begin{bmatrix} (-) \\ (+) \\ (+) \end{bmatrix}$	$\begin{bmatrix} (-) \\ (-) \\ (-) \end{bmatrix}$	$\begin{bmatrix} (+) \\ (-) \\ (+) \end{bmatrix}$
$\boldsymbol{E}$	$\begin{bmatrix} (-) \\ (+) \\ (+) \end{bmatrix}$	$\begin{bmatrix} (-) \\ (-) \\ (-) \end{bmatrix}$	$\begin{bmatrix} (-) \\ (+) \\ (-) \end{bmatrix}$

pendicular to $\boldsymbol{n}$ are zero. The choice of $v_1 = 0$ (hard wall) again prevents a flux density of pressure and kinetic energy (Eq. (32)) across the boundary. For $\boldsymbol{B}$, all the components have (+) symmetry. The symmetries are given in Table 2 for this case under the heading $\boldsymbol{n} = \boldsymbol{e}_1$ Conductor. The symmetry of $\boldsymbol{J}$ is not well determined, since from Ampere's Law Eq. (27),

$$\boldsymbol{J} = \nabla \times \boldsymbol{B} = \begin{bmatrix}(-)\\(+)\\(+)\end{bmatrix} \times \begin{bmatrix}(+)\\(+)\\(+)\end{bmatrix} = \begin{bmatrix}(+)\\(\pm)\\(\pm)\end{bmatrix}, \tag{43}$$

with $(\pm)$ indicating a mixed symmetry. Fortunately, the momentum equation is not needed at the boundary ($\boldsymbol{v} = 0$), and there are no derivatives of $\boldsymbol{J}$ in the equations. The authors have successfully used this boundary condition in simulations of magnetospheric Alfvén waves [10,6,7], indicating that this boundary condition works despite the imperfect symmetries.

3.3. Hard wall perfect conducting boundary with $\boldsymbol{n} = \boldsymbol{e}_2$ (perpendicular to $\boldsymbol{b}_0$)

Again, we want the components of $\boldsymbol{E}$ perpendicular to $\boldsymbol{n}$ to be zero and the component v_2 (parallel to $\boldsymbol{n}$) equal to zero in order that the flux density of energy ($\boldsymbol{S}$ in Eq. (32)) has no component across the boundary. In this case, all the symmetries are consistent, as shown in Table 2. For a hard wall perfect conductor boundary with $\boldsymbol{n} = \boldsymbol{e}_3$, one can simply interchange the symmetries of the second and third components.

4. Energy conserving boundary conditions for a hybrid code

Normalized hybrid code equations for two species, particle protons (p) and fluid electrons (e) [27], are written as

$$\frac{d\boldsymbol{v_m}}{dt} = \boldsymbol{E_m} - \eta \boldsymbol{J_m} + \boldsymbol{v_m} \times \boldsymbol{B_m}, \tag{44}$$

$$\frac{d\boldsymbol{x_m}}{dt} = \boldsymbol{v_m}, \tag{45}$$

$$n_{ei} = n_{pi} = \frac{W}{V_i} \sum_m S(\boldsymbol{x_i} - \boldsymbol{x_m}), \tag{46}$$

$$\boldsymbol{J_{pi}} = \frac{W}{V_i} \sum_m \boldsymbol{v_m} S(\boldsymbol{x_i} - \boldsymbol{x_m}), \tag{47}$$

$$\boldsymbol{J_i} = \nabla \times \boldsymbol{B_i}, \tag{48}$$

$$\boldsymbol{v_{ei}} = \frac{Q}{n_{ei}} (\boldsymbol{J_{pi}} - \boldsymbol{J_i}), , \tag{49}$$

$$\frac{\partial p_{ei}}{\partial t} = -\gamma \nabla \cdot (\boldsymbol{v_{ei}} p_{ei}) - (1-\gamma) \boldsymbol{v_{ei}} \cdot \nabla p_{ei} + (\gamma - 1) \eta J_i^2, \tag{50}$$

$$\frac{\partial \boldsymbol{B_i}}{\partial t} = -\nabla \times \boldsymbol{E_i}, \tag{51}$$

$$\boldsymbol{E_i} = -\boldsymbol{v_{ei}} \times \boldsymbol{B_i} + \eta \boldsymbol{J_i}, \tag{52}$$

where m is the particle index, i is the grid index (possibly representing grid points on a multidimensional grid), the particle weight $W = (\sum_i V_i)/N_m, V_i$ is the volume of grid cell i, and N_m is the number of particles. The particle quantities are the particle position $\boldsymbol{x_m}$ and the particle velocity $\boldsymbol{v_m}$. If the coordinates are curved, the particle acceleration equation Eq. (44) must also include (centrifugal and Coriolis) inertial terms as discussed by Lipatov [16].

The normalized particle charge Q (normally unity) will be discussed below. Other quantities are fields evaluated on the grid. Fields with a subscript m (like $\boldsymbol{E_m}$) are understood to be interpolated to the particle position like

$$\boldsymbol{E_m} = \sum_i \boldsymbol{E_i} S(\boldsymbol{x_i} - \boldsymbol{x_m}) \tag{53}$$

using the particle shape function $S(\boldsymbol{x_i} - \boldsymbol{x_m})$. The normalizations are similar to those of MHD except that time is normalized to the inverse proton cyclotron frequency $\Omega_{cp} = eB_0/m_p$, where m_p is the proton mass, and distances are normalized to c/ω_{pp}, and where the proton plasma frequency $\omega_{pp} = \sqrt{n_0 e^2/(\epsilon_0 m_p)}$, where ϵ_0 is the permittivity of free space.

The energy equation is

$$\frac{\partial}{\partial t}\mathcal{E} = -\sum_i V_i \nabla \cdot \boldsymbol{S}, \tag{54}$$

$$\mathcal{E} = \sum_m \frac{W|\boldsymbol{v_m}|^2}{2} + \sum_i V_i \left(\frac{p_{ei}}{\gamma - 1} + \frac{|\boldsymbol{B_i}|^2}{2} \right), \tag{55}$$

$$\boldsymbol{S} = \left(\boldsymbol{v_{ei}} \frac{\gamma p_e}{\gamma - 1} + \boldsymbol{E} \times \boldsymbol{B} \right). \tag{56}$$

Here in Eq. (55), the particle energy (summed over m) does not easily separate from the field energy (summed over i), so we have written the energy in nonlocal terms (in terms of sums, unlike Eq. (32)). We still need to have $\boldsymbol{S}\cdot\boldsymbol{n}=0$ at the boundary for energy conservation. In addition, we need to handle particle interactions at the boundary in an energy conserving way. The particles are normally reflected at the boundary with the normal component of velocity ($\boldsymbol{v_m}\cdot\boldsymbol{n}$) reversed [3]. Another possibility is to reverse all components of the particle velocity upon reflection, or the normal component plus any component within the boundary perpendicular to $\mathbf{B}$ [20]. For our purposes, we will assume that the particles are reflected when they hit the boundary with only the normal component of velocity reversed. The reversal of a component of particle velocity will be indicated by $(-)$ symmetry.

Our boundary conditions for the hybrid code are shown in Table 3. They are quite similar to those we derived for MHD (Table 2). For the insulator boundary at the boundary with $\boldsymbol{n}=\boldsymbol{e}_1$, the symmetries in the hybrid system are totally consistent. This boundary condition was used in the simulation of flux bundle reconnection of Mandt et al. [19]. For the conductor boundary with boundary normal across the magnetic field ($\boldsymbol{n}=\boldsymbol{e}_2$), the boundary conditions are consistent only if the particle charge Q in Eq. (49) has $(-)$ symmetry. That is, $Q=0$ at the radial boundary. This reversal of the charge is consistent with the reflection of the protons we have assumed at the boundary (see Fig. 1), and also with the fact that $\nabla\cdot\boldsymbol{E}$, proportional to the charge density according to Gauss's Law, has $(-)$ symmetry at the boundary.

Fig. 2 shows the change in the total energy $\delta\mathcal{E}$ (from the beginning of the simulation) for a 2D simulation of electromagnetic ion cyclotron waves in dipole geometry using conductor boundary conditions for both $\boldsymbol{n}=\boldsymbol{e}_1$ and $\boldsymbol{n}=\boldsymbol{e}_2$ (Table 3). The electromagnetic ion cyclotron instability is driven by the temperature anisotropy, $T_\perp > T_\parallel$, of the ions. The simulation domain extends along the magnetic equator from $L=40$ to 60 c/ω_{pp} away from the center of the Earth, and the central magnetic field line (at $L=50c/\omega_{pp}$) extends in latitude to $\pm 45^\circ$. The grid resolution was 129 grid points in the parallel direction and 33 in the perpendicular (along L) direction. (This simulation will be described further elsewhere.) The energy is defined as in Eq. (55), except that it has been integrated over the system volume. Fig. 2 also shows the change in the magnetic energy (term proportional to $|\boldsymbol{B_i}|^2$ in Eq. (55)) and the kinetic energy (term proportional to $|\boldsymbol{v_m}|^2$ in Eq. (55)). The fact that the change in the total energy is much smaller than the change in the individual energy terms $\delta\mathcal{E}_B$ and $\delta\mathcal{E}_K$ shows that the energy was

Table 3
Symmetries for energy conserving boundary conditions for a hybrid code.

Field	$\boldsymbol{n}=\boldsymbol{e}_1$		$\boldsymbol{n}=\boldsymbol{e}_2$
	Insulator	Conductor	Conductor
p_e, h_1, h_2, h_3	(+)	(+)	(+)
Q	(+)	(+)	(−)
$\mathbf{V}$	$\begin{bmatrix}(-)\\(+)\\(+)\end{bmatrix}$	$\begin{bmatrix}(-)\\(+)\\(+)\end{bmatrix}$	$\begin{bmatrix}(+)\\(-)\\(+)\end{bmatrix}$
$\boldsymbol{B}$	$\begin{bmatrix}(+)\\(-)\\(-)\end{bmatrix}$	$\begin{bmatrix}(+)\\(+)\\(+)\end{bmatrix}$	$\begin{bmatrix}(+)\\(-)\\(+)\end{bmatrix}$
$\boldsymbol{J_{pi}}, \boldsymbol{J}$	$\begin{bmatrix}(-)\\(+)\\(+)\end{bmatrix}$	$\begin{bmatrix}(+)\\(\pm)\\(\pm)\end{bmatrix}$	$\begin{bmatrix}(-)\\(+)\\(-)\end{bmatrix}$
$\mathbf{v_{ei}}, \boldsymbol{v_m}$	$\begin{bmatrix}(-)\\(+)\\(+)\end{bmatrix}$	$\begin{bmatrix}(-)\\(+)\\(+)\end{bmatrix}$	$\begin{bmatrix}(+)\\(-)\\(+)\end{bmatrix}$
$\boldsymbol{E}$	$\begin{bmatrix}(-)\\(+)\\(+)\end{bmatrix}$	$\begin{bmatrix}(-)\\(-)\\(-)\end{bmatrix}$	$\begin{bmatrix}(-)\\(+)\\(-)\end{bmatrix}$

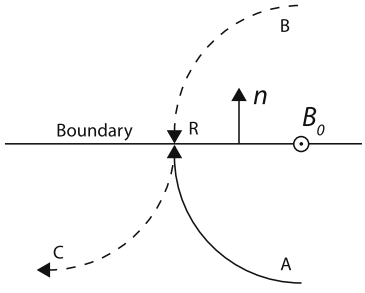

Fig. 1. Particle reflection illustrated for a conductor boundary with boundary normal across the magnetic field ($\boldsymbol{n}=\boldsymbol{e}_2$). Particle A reflects at point R, implying that there is an image particle with opposite charge B (rotating with the opposite sense of rotation) that crosses the boundary at point R and becomes particle C.

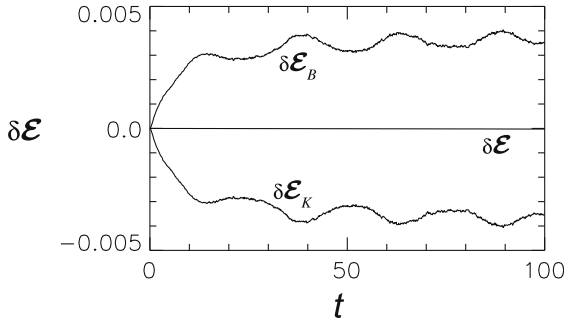

Fig. 2. The change (from the beginning of the simulation) in the magnetic field energy $\delta\mathcal{E}_B$, the change in the kinetic energy $\delta\mathcal{E}_K$, and the change in the total energy $\delta\mathcal{E} = \delta\mathcal{E}_B + \delta\mathcal{E}_K$, versus time for a 2D hybrid code simulation of electromagnetic ion cyclotron waves in dipole coordinates. The starting magnetic energy was 6.7 while the initial kinetic energy was 0.70. (The energies are volume averaged so that the magnetic energy would be unity if the magnetic field were of uniform magnitude.)

well conserved in this simulation; the small (slightly negative) change in the total energy can be reduced by using higher grid resolution with a smaller time step.

5. Energy conserving boundary conditions for linear reduced MHD

Now we consider a simple set of linear reduced MHD (RMHD) equations

$$\frac{\partial A_\parallel}{\partial t} = -\boldsymbol{b}_0 \cdot \nabla\phi, \tag{57}$$

$$J_\parallel = -\frac{1}{B_0}\nabla \cdot \left(\nabla_\perp\left(\frac{A_\parallel}{B_0}\right)B_0^2\right), \tag{58}$$

$$\nabla \cdot \left(\frac{1}{V_A^2}\frac{\partial \nabla_\perp \phi}{\partial t}\right) = \boldsymbol{B}_0 \cdot \nabla\left(\frac{J_\parallel}{B_0}\right), \tag{59}$$

where the electromagnetic fields are

$$\boldsymbol{B}_\perp = \nabla \times (\boldsymbol{b}_0 A_\parallel) = \nabla\left(\frac{A_\parallel}{B_0}\right) \times \boldsymbol{B}_0, \tag{60}$$

$$\boldsymbol{E} = -\nabla\phi - \boldsymbol{b}_0 \frac{\partial A_\parallel}{\partial t}, \tag{61}$$

and the equations have been written in a form valid for curvilinear coordinates with $\boldsymbol{b}_0 = \boldsymbol{B}_0/B_0 = \boldsymbol{e}_1$, but assuming $\boldsymbol{J}_0 = \nabla \times \boldsymbol{B}_0 = 0$. The $\parallel$ and $\perp$ subscripts indicate components respectively parallel and perpendicular to the background magnetic field $\boldsymbol{B}_0$. We define $L_\parallel$ and $L_\perp$, the parallel and perpendicular scale lengths. In Eqs. (57)–(61), $A_\parallel$ is normalized to $B_0 L_\perp$, and $\partial/\partial t$ is normalized to $V_{A0}/L_\parallel$, and V_A is normalized to $V_{A0} = V_A$ at a particular location. Eq. (57) indicates that the parallel electric field $E_\parallel = \boldsymbol{b}_0 \cdot \boldsymbol{E} = 0$; Eq. (58) is Ampere's Law for the parallel current $J_\parallel = \boldsymbol{b}_0 \cdot \boldsymbol{J}$ with $\boldsymbol{J} = \nabla \times \boldsymbol{B}$ using Eq. (60) (and $\boldsymbol{J}_0 = 0$); and Eq. (59) expresses current continuity, where the left-hand side of the equation is the negative of the divergence of the perpendicular current due to the polarization drift and the right-hand side of the equation is the divergence of the parallel current $J_\parallel \boldsymbol{b}_0$ (so that the divergence of the total current is zero).

Defining

$$A' = \frac{A_\parallel}{B_0}, \tag{62}$$

$$J' = \frac{J_\parallel}{B_0}, \tag{63}$$

we can rewrite Eqs. (57)–(59) as

$$\frac{\partial A'}{\partial t} = -\frac{1}{B_0}\boldsymbol{b}_0 \cdot \nabla\phi, \tag{64}$$

$$J' = -\frac{1}{B_0^2}\nabla \cdot \left(B_0^2 \nabla_\perp A'\right), \tag{65}$$

$$\nabla \cdot \left(\frac{1}{V_A^2}\frac{\partial \nabla_\perp \phi}{\partial t}\right) = \boldsymbol{B}_0 \cdot \nabla J', \tag{66}$$

and Eqs. (60) and (61) as

$$\boldsymbol{B}_\perp = \nabla A' \times \boldsymbol{B}_0, \tag{67}$$

$$\boldsymbol{E} = -\nabla\phi - \boldsymbol{B}_0 \frac{\partial A'}{\partial t}. \tag{68}$$

The energy principle corresponding to Eqs. (64)–(66) is

$$\frac{\partial}{\partial t}\mathcal{E} = -\nabla\cdot\boldsymbol{S}, \tag{69}$$

$$\mathcal{E} = \frac{|\nabla_\perp\phi|^2}{2V_A^2} + \frac{\boldsymbol{B}_\perp^2}{2}, \tag{70}$$

$$\boldsymbol{S} = \boldsymbol{B}_0 J'\phi - \nabla_\perp A' \frac{\partial A'}{\partial t} B_0^2 - \frac{\phi}{V_A^2}\nabla_\perp \frac{\partial\phi}{\partial t}, \tag{71}$$

Note that $|\nabla_\perp\phi|^2/2V_A^2 = \rho v_E^2/2$, where

$$\boldsymbol{v}_{\boldsymbol{E}} = (-\nabla\phi \times \boldsymbol{b}_0)/B_0 \tag{72}$$

is the $\boldsymbol{E}\times\boldsymbol{B}$ drift velocity. Note also that this form for the $\boldsymbol{E}\times\boldsymbol{B}$ drift has been assumed also in the polarization drift current in Eq. (59) (which does not have $\boldsymbol{E}\times\delta\boldsymbol{B}$).

5.1. Reduced MHD boundary conditions for $\boldsymbol{n} = \boldsymbol{e}_1$

First we consider the boundary crossed along the background magnetic field, that is, boundary normal $\boldsymbol{n} = \boldsymbol{e}_1 = \boldsymbol{b}_0$. Energy conserving boundary conditions for RMHD are summarized in Table 4. The insulator boundary condition 1 in Table 4 allows an electric field within the boundary, but not a magnetic field. Therefore ϕ can be nonzero within the boundary ($\rightarrow \nabla_2\phi \neq 0$ and $\nabla_3\phi \neq 0$ within the boundary), but A' must be zero within the boundary. The resulting boundary conditions are exactly the same as those for the corresponding boundary condition in MHD (Table 2) except that from Eq. (72), $v_1 = v_\parallel = 0$. A more general set of RMHD equations including nonzero v_1 [4,8] would have exactly the same set of symmetries as in MHD.

Now we consider a conducting boundary crossed in the $\boldsymbol{e}_1$ direction ($\boldsymbol{n} = \boldsymbol{e}_1$). In 3D ($\nabla_3 \neq 0$), the symmetries are again mixed. To simplify the discussion, we consider the 2D case, $\nabla_3 = 0$, for which the symmetries are consistent. Two dimensional reduced MHD equations (with $\boldsymbol{b}_0 = \boldsymbol{e}_1$) have been used in simulations of Auroral Alfvén waves by Refs. [23,17,22]. While the equations of these authors are more complicated than Eqs. (64)–(66), Eqs. (64)–(66) represent the fundamental physics of Alfvén waves within the more complicated sets of equations. The symmetries for the 2D conducting boundary with $\boldsymbol{n} = \boldsymbol{e}_1$ are shown in Table 4 (boundary condition 2). Note that

$$\nabla = \begin{bmatrix} (-) \\ (+) \\ 0 \end{bmatrix} \tag{73}$$

indicates that the third component of ∇ is identically zero. Now a magnetic field is allowed within the boundary but not an electric field, so A' can be nonzero within the boundary but $\phi = 0$ there. Because of this, $E_\parallel = \boldsymbol{b}_0\cdot\boldsymbol{E}$ has (+) symmetry (sym-

Table 4
Symmetries for energy conserving boundary conditions for linear reduced MHD.

Field	$\boldsymbol{n} = \boldsymbol{e}_1$			$\boldsymbol{n} = \boldsymbol{e}_2$	
	1-Insulator	2-Conductor	3-Grounded	4-Ground/zero slope	5-Ground/zero 2nd derivative
$B_0, V_A,$	(+)	(+)	(+)	(+)	(+)
h_1, h_2, h_3	(+)	(+)	(+)	(+)	(+)
ϕ	(+)	(−)	(−)	(+0)/(+)	(−)/(δ−)
A'	(−)	(+)	(−)	(+0)/(+)	(−)/(δ−)
∇	$\begin{bmatrix}(-)\\(+)\\(+)\end{bmatrix}$	$\begin{bmatrix}(-)\\(+)\\0\end{bmatrix}$	$\begin{bmatrix}(+)\\(-)\\(+)\end{bmatrix}$	$\begin{bmatrix}(+)\\(-)\\0\end{bmatrix}$	$\begin{bmatrix}(+)\\(-)\\0\end{bmatrix}$
$\boldsymbol{B}$	$\begin{bmatrix}(+)\\(-)\\(-)\end{bmatrix}$	$\begin{bmatrix}(+)\\0\\(+)\end{bmatrix}$	$\begin{bmatrix}(+)\\(-)\\(+)\end{bmatrix}$	$\begin{bmatrix}(+)\\0\\(-)\end{bmatrix}$	$\begin{bmatrix}(+)\\0\\(+)\end{bmatrix}$
J'	(−)	(+)	(−)	(+)	(−)
$\boldsymbol{v}$	$\begin{bmatrix}0\\(+)\\(+)\end{bmatrix}$	$\begin{bmatrix}0\\(-)\\(-)\end{bmatrix}$	$\begin{bmatrix}0\\(-)\\(+)\end{bmatrix}$	$\begin{bmatrix}0\\0\\(-)\end{bmatrix}$	$\begin{bmatrix}0\\(-)\\(+)\end{bmatrix}$
$\boldsymbol{E}$	$\begin{bmatrix}(-)\\(+)\\(+)\end{bmatrix}$	$\begin{bmatrix}(+0)\\(-)\\(-)\end{bmatrix}$	$\begin{bmatrix}(-)\\(+)\\(-)\end{bmatrix}$	$\begin{bmatrix}(+0)\\(-)\\0\end{bmatrix}$	$\begin{bmatrix}(-)\\(+)\\0\end{bmatrix}$

metry of A' and $\nabla_1\phi$), but $E_\parallel = 0$ from Eq. (57), so we indicate the symmetry of $E_1 = E_\parallel$ as (+0) in Table 4. This notation denotes zero value with (+) symmetry (value $\propto x^2$ at boundary coordinate $x = 0$). Apart from this difference (we chose $(-)$ symmetry for E_1 in Table 2), the symmetries of the nonzero components are identical to those for MHD in Table 2.

5.2. Reduced MHD boundary conditions for $\boldsymbol{n} = \boldsymbol{e}_2$

Now we consider the boundary crossed when moving perpendicular to the magnetic field, $\boldsymbol{n} = \boldsymbol{e}_2$. In Sections 3 and 4 we described a conducting boundary. The simplest way to create a conducting boundary in RMHD is to ground the boundaries so that $\phi = 0$ there and the symmetry of ϕ is $(-)$. Then since $\nabla_1\phi = 0$ within that boundary ($\boldsymbol{e}_1 = \boldsymbol{b}_0$ is within the boundary perpendicular to $\boldsymbol{n} = \boldsymbol{e}_2$), $\partial A'/\partial t = 0$ from Eq. (64), so that the symmetry of A' is also $(-)$. This leads to a consistent set of boundary conditions which is described in Table 4 under boundary condition 3. In a more general set of equations including $v_1 = v_\parallel$ [4,8], the symmetry of v_1 would be (+) so that (as in MHD), the symmetry of $\boldsymbol{v}$ is the same as that of $\boldsymbol{B}$ (Table 2). Note that in this case, the symmetry of v_1 would be opposite to that of J' ($(-)$ in Table 4), as is also the case in MHD (Table 2). But in the equations of Refs. [4,8], $J_\parallel$ is equal to the current of the protons minus that of the electrons (as it must be in reality), $q_p n_p v_{\parallel p} - e n_e v_{\parallel e}$. This apparent contradiction (opposite symmetry for $v_\parallel$ and $J' \propto J_\parallel$) can be resolved if the charge has $(-)$ symmetry as we assumed for the hybrid code. Again, the assumption that there is no charge at the boundary is consistent with $\nabla \cdot \boldsymbol{E} = 0$, which is true for the conducting boundary. The double ground radial boundary condition has been used by Streltsov and Lotko [23].

While grounding the boundary is a simple way to implement a conducting boundary, constraining the value of ϕ at both ends of the simulation alters the Alfvén wave dynamics so that an Alfvén wave energy is no longer purely guided along the magnetic field [9]. (The negative effect of this boundary condition did not invalidate the main results of Streltsov and Lotko [23] because they were concentrating on fine scale structure that develops near the ionospheric boundary due to other mechanisms.) For ease of discussion, we now consider q and r to be the (possibly curvilinear) coordinates in the $\boldsymbol{e}_1$ and $\boldsymbol{e}_2$ directions, respectively. The coordinate r will play the role of x that we used previously; that is, increasing values of r will cross the boundary. To solve the problem mentioned above (incorrect Alfvén wave dynamics), we can use a slightly different boundary condition for the low and high end of the r boundary. Because Eq. (66) must be inverted to get ϕ, and only the perpendicular gradient of ϕ appears in Eq. (66), the solution for ϕ includes an arbitrary constant. Because of this, we set $\phi = 0$ at the low end of the r boundary, $r = r_1$. Then from Eq. (57), $A_\parallel$ is also zero there. We will not require that $\phi = 0$ at the high end of the r boundary, $r = r_2$, for boundary conditions 4 and 5. With a gauge transformation, it is possible to transform to a different Φ and $A_\parallel$ such that $\Phi = A_\parallel = 0$ at $r = r_2$. This transformation is $\Phi \to \Phi - \partial\psi/\partial t$ and $A_\parallel \to A_\parallel + \boldsymbol{b}_0 \cdot \nabla\psi$ with $\psi = \int^t dt' \Phi(q, r = r_2, t')$. Thus the boundary conditions at $r = r_1$ and $r = r_2$ are physically equivalent for all the boundary conditions.

To indicate the different way this boundary is handled at $r = r_1$ and $r = r_2$, the symmetry of ϕ in Table 4 is listed for boundary condition 4 as (+0)/(+) where the '/' separates the boundary conditions at $r = r_1$ and $r = r_2$, respectively. This means that at the r_1 boundary, $\phi = 0$ but with (+) symmetry, while at the r_2 boundary, the value of ϕ is allowed to float with (+) symmetry. The symmetries of the other fields are given in Table 4. This boundary condition is partly like a conductor (the components of $\boldsymbol{E}$ within the boundary are zero) only because of the 2D approximation. The symmetries of E_2 and B_3 are those of an insulator. The symmetries of the fields are consistent only in 2D.

Boundary condition 5 (Table 4) is more like that of the MHD conducting boundary in Table 2. For this boundary condition, the notation $(\delta-)$ indicates that the variations in the r direction are antisymmetric about a nonzero value. This means that ϕ can be nonzero at $r = r_2$, but $\phi(q, r) - \phi(q, r = r_2)$ has $(-)$ symmetry. This boundary condition leads to zero value for $\partial^2\phi/\partial dr^2 \propto \partial E_r/\partial r$, which is the MHD boundary condition for $E_r = E_2$ (Table 2). The symmetries of the other fields are also consistent with MHD. (One must apply the $\delta-$ symmetry to A' rather than A, or the product $A(1/B_0)$ in Eq. 58 will have the wrong symmetry before the derivative in $\nabla_\perp$ is taken.)

There is a subtle problem implementing boundary condition 5. With the symmetries in Table 4, the right-hand side of Eq. (66) will have $(-)$ symmetry and zero value at $r = r_2$, and Eq. (66) will turn into $\partial^2\phi/\partial dr^2 = 0$. But this is exactly equivalent to the boundary condition for ϕ, and Eq. (66) yields no new information to determine ϕ at $r = r_2$ [the solution for ϕ is singular]. One possible way to deal with this is to drop the (+) symmetry for the equilibrium quantities B_0, V_A, h_1, h_2, and h_3. The energy conservation will not then be exact. If we understand them correctly, researchers at the University of Alberta have chosen $(\delta-)$ for the symmetry of A', but (+) for the symmetry of ϕ [Robert Rankin, private communication, 2007].

6. Summary and discussion

We have shown how to implement energy conserving boundary conditions using exact symmetries at the boundaries. This method can be used even for a curvilinear coordinate system if the symmetries are exact. (When equations do not have exact symmetries, it is usually better to let the equilibrium quantities and scale factors be continuous at the boundary.) We demonstrated how to work out the symmetries of the various fields for MHD, a hybrid code, and for linear reduced MHD.

In Section 2, we mentioned that perfect (+) or (-) symmetries across a boundary imply that all odd or even derivatives are equal to zero. One might be concerned about the high order derivatives which are implied by multiple ghost grid points (or cells) beyond the boundary. Analytically, either a Dirichlet or Neumann boundary condition is sufficient at boundaries. If we

specify only that the slope is zero at a boundary, but have more than one ghost grid point value beyond that boundary, there is an infinite number of ways to adjust the ghost values and still have zero slope. Given this flexibility, to extend the ghost grid point values using symmetry seems a reasonable thing to do. And symmetries provide a sufficient condition for energy conservation (as far as the boundary is concerned). But such symmetries are probably not the only way to achieve energy conservation (not a necessary condition for energy conservation). One could set the ghost values in different ways, perhaps to set high order derivatives to zero. Alternately, one could use lower order one-sided derivatives requiring fewer input values as the boundary is approached. This would eliminate the extra degrees of freedom, but the energy would likely not be conserved. Ultimately, one always makes a choice about how to handle the boundaries that involves certain assumptions, and may not be totally realistic. For instance, the assumption of periodic boundary conditions assumes exact periodicity that is unlikely in a real system. But we make a choice to use certain boundary conditions that has the properties that we desire. If exact energy conservation is desired, then the symmetry boundary conditions described here are one way to achieve it.

Acknowledgments

Work at Dartmouth was supported by NSF grants ATM-0503371 and ATM-0120950 (Center for Integrated Space Weather Modeling, CISM, funded by the NSF Science and Technology Centers Program) and NASA grant NNX08AI36G (Heliophysics Theory Program). RED especially thanks James F. Drake for introducing him to symmetry boundary conditions. We also thank John Lyon, Jan Hesthaven, and Alain Brizard for helpful discussions.

References

[1] G. Arfken, Mathematical Methods for Physicists, second ed., Academic Press, New York, 1970 (Chapter 2).
[2] I.B. Bernstein, E.A. Frieman, M.D. Kruskal, R.M. Kulsrud, Proc. Roy. Soc. London, Ser. A 244 (1236) (1958) 17–40.
[3] C.K. Birdsall, A.B. Langdon, Plasma Physics via Computer Simulation, McGraw-Hill, New York, 1985.
[4] A.J. Brizard, Phys. Plasmas 12 (9) (2005) 092302-1–092302-11.
[5] W. Daughton, J. Scudder, H. Karimabadi, Phys. Plasmas 13 (2006) 072101.
[6] R.E. Denton, G. Vetoulis, J. Geophys. Res. 103 (1998) 6729.
[7] R.E. Denton, D.-H. Lee, K. Takahashi, J. Goldstein, R. Anderson, J. Geophys. Res. 107 (A7) (2002), doi:10.1029/2001JA000272.
[8] R.E. Denton, B. Rogers, W. Lotko, Phys. Plasmas 14 (2007) 102906, doi:10.1063/1.2786060.
[9] R.E. Denton, B. Rogers, W. Lotko, Anatoly Streltsov, Phys. Plasmas 15 (2008) 032106, doi:10.1063/1.2898409.
[10] D.Q. Ding, R.E. Denton, M.K. Hudson, R.L. Lysak, J. Geophys. Res. 100 (1995) 63.
[11] C.T. Dum, in: H. Matsumoto, T. Sato, Computer Simulation of Space Plasmas, Terra, Tokyo, 1985 (page 303).
[12] T.G. Forbes, E.R. Priest, Rev. Geophys. 25 (8) (1987) 1583–1607.
[13] J.D. Jackson, Classical Electrodynamics, second ed., John Wiley and Sons, New York, 1995 (Chapter 11);
A.S. Lipatov, The hybrid multiscale simulation technology: an introduction with application to astrophysical and laboratory plasmas, Springer, Berlin, 2002 (Chapter 3).
[14] D.-H. Lee, K.-H. Kim, R.E. Denton, K. Takahashi, Earth Planets Space 56 (2004) e33–e36.
[15] R.J. Leveque, Finite Volume Methods for Hyperbolic Problems, Cambridge University Press, Cambridge, 2002.
[16] A.S. Lipatov, The hybrid multiscale simulation technology: an introduction with application to astrophysical and laboratory plasmas, Springer, Berlin, 2002 (Chapter 3).
[17] J.Y. Lu, R. Rankin, R. Marchand, V.T. Tikhonchuk, Geophys. Res. Lett. 30 (10) (2003) 1540, doi:10.1029/2003GL016929.
[18] J.G. Lyon, J.A. Fedder, C.M. Mobarry, J. Atmos. Sol-Terr. Phys. 66 (15–16) (2004) 1333–1350.
[19] M.E. Mandt, R.E. Denton, J.F. Drake, Geophys. Res. Lett. 21 (1994) 73.
[20] H. Naitou, S. Tokuda, T. Kamimura, J. Comput. Phys. 33 (1979) 86–101.
[21] W.M. Nevins, Y. Matsuda, M.J. Gerver, J. Comput. Phys. 39 (1) (1981) 226–232.
[22] R. Rankin, J.Y. Lu, R. Marchand, E.F. Donovan, Phys. Plasmas 11 (4) (2004) 1268, doi:10.1063/1.1647138.
[23] A.V. Streltsov, W. Lotko, J. Geophys. Res. 108 (A7) (2003) 1289, doi:10.1029/2002JA009806.
[24] D.W. Swift, in: H. Usui, Y. Omura (Eds.), Advanced Methods for Space Simulations, TERRAPUB, Tokyo, 2007, pp. 77–89.
[25] T. Tajima, Computational Plasma Physics: With Applications to Fusion and Astrophysics, Addison-Wesley, Redwood City, California, 1989.
[26] D. Winske, N. Omidi, J. Geophys. Res. 101 (A8) (1996) 17. 287.
[27] D. Winske, L. Yin, N. Omidi, H. Karimabadi, K. Quest, in: J. Buchner, C.T. Dum, M. Scholer (Eds.), Space Plasma Simulation, Springer, Berlin, 2003, p. 136.
[28] S.T. Zalesak, J. Comput. Phys. 40 (2) (1981) 508.